RESEARCH ARTICLE

Isothiourea-Catalyzed Atropselective Acylation of Biaryl Phenols via Sequential Desymmetrization / Kinetic Resolution

Elizabeth S. Munday,[a] Markas A. Grove,[b] Taisiia Feoktistova,[b] Alexander C. Brueckner,[b] Daniel Walden,[b] Claire M. Young,[a] Alexandra M. Z Slawin,[a] Andrew D. Campbell,[c] Paul Ha-Yeon Cheong*[b] and Andrew D. Smith*[a]

Abstract: Axially chiral phenols are attractive targets in organic synthesis. This motif is central to many natural products and widely used as precursors to, or directly, as chiral ligands and catalysts. Despite their utility few simple catalytic methods are available for their synthesis in high enantiopurity. Herein the atropselective acylation of a range of symmetric biaryl diols is investigated using isothiourea catalysis. Studies on a model biaryl diol substrate shows that the high product er observed in the process is a result of two successive enantioselective reactions consisting of an initial enantioselective desymmetrization coupled with a second chiroablative kinetic resolution. Extension of this process to a range of substrates, including a challenging tetraorthosubstituted biaryl diol, led to highly enantioenriched products (14 examples, up to 98:2 er), with either HyperBTM or BTM identified as the optimal catalyst depending upon the substitution pattern within the substrate. Computation has been used to understand the factors that lead to high enantiocontrol in this process, with maintenance of planarity to maximize a 1,5-S•••O interaction within the key acyl ammonium intermediate identified as the major feature that determines atropselective acylation and thus product enantioselectivity.

Introduction

The development of methods for the enantioselective preparation of configurationally stable chiral biaryls has been developed widely in recent years.[1] Various catalytic strategies have been developed in this area,[2] with the most common approaches falling into three distinct categories that involve direct coupling, dynamic kinetic resolution (DKR), or desymmetrization.[1] Direct enantioselective coupling of two aromatic fragments to give biaryls is a well-established method, as demonstrated in seminal work from Buchwald using an enantioselective Suzuki coupling,[3] and more recently by Tang in the synthesis of Michellamine B.[4] However, the coupling of two inherently hindered fragments in this strategy often requires prohibitively expensive ligands and is typically restricted to specific systems. DKR approaches,[1,5] which install a steric barrier to rotation, are common. Notable catalytic approaches include Miller's enantioselective bromination approach,[6] and Turner and Clayden's biocatalytic transfer hydrogenation,[7] among others.[8] Desymmetrization represents an alternative and attractive strategy to the synthesis of chiral biaryls, as complexity can be introduced in a single atropselective step.[9] A limited number of processes have been developed that use this strategy,[10] with the current state-of-the-art represented by the bromination approach of Akiyama,[11] the cross-coupling approaches of Hayashi,[12,13] and the organocatalytic S_NAr approach reported by Smith (Figure 1A).[14]

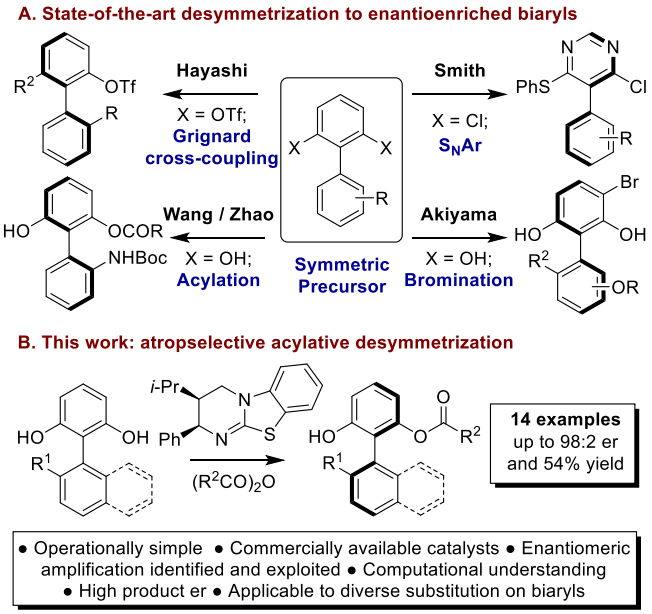

Figure 1. Overview of state-of-the-art desymmetrization approaches for the synthesis of enantioenriched biaryls

Lewis base-catalyzed enantioselective acylative kinetic resolution has recently been exploited by Sibi, Zhao and ourselves for the synthesis of enantioenriched biaryls.[15-18] At the onset of these studies the acylative desymmetrization of biaryl phenols using a small molecule catalyst had not been demonstrated.[19] In recent independent publications, Wang and Zhao disclosed the desymmetrization of biaryl amino alcohol derivatives via NHC-catalyzed acylation.[20] Despite both giving excellent product enantioselectivity, the scope was limited to amino-alcohol substrates, and the process required high catalyst loadings (10-20 mol% azolium salt precatalysts) and either a co-oxidant or excess acylating agent (2.5 equiv.) for optimal results. Isothioureas have been extensively exploited as mild, readily available chiral Lewis bases.[21] They are recognized as effective catalysts for the acylative kinetic resolution (KR) of point chiral primary,[22] secondary,[23] and tertiary alcohols,[24] and the acylative desymmetrization of diols.[25] Building upon our work on enantioselective acyl transfer using isothiourea catalysis,[18] we considered the generation of atropisomeric species through the acylative desymmetrization of symmetric biaryl diols (Figure 1B). We set out to deliver a process that would be applicable to a diverse scope of biaryls, without the requirement of incorporating

[a] E. S. Munday, Dr. C. M. Young, Prof. A. M. Z. Slawin, Prof. A. D. Smith, EaStCHEM School of Chemistry, University of St Andrews, North Haugh, St Andrews, KY16 9ST (UK)
E-mail: ads10@st-andrews.ac.uk
[b] M. A. Grove, T. Feoktistova, A. C. Breukner, D. M. Walden, Prof. P. H.-Y.Cheong
Department of Chemistry, Oregon State University, 153 Gilbert Hall, Corvallis, OR 97331 (USA) E-mail: cheongh@oregonstate.edu
[c] Dr A. D. Campbell
Pharmaceutical Technology and Development, AstraZeneca, Silk Road Business Park, Macclesfield, Cheshire, SK10 2NA, UK
Supporting information for this article is given via a link at the end of the document.

a directing group, such as that utilized in the previous work of Akiyama (an ether) or Wang and Zhao (N-protected aniline). In this manuscript this strategy is applied to the synthesis of a range of highly enantioenriched biaryls. Detailed experimental and computational studies show that this process proceeds through two successive atropselective steps, consisting of an initial desymmetrization followed by a kinetic resolution process, with enantiomeric amplification[26] decisive in determining the product configuration in these processes. For a model diol substrate, computational analysis has determined the structural factors and key interactions that lead to high product enantiocontrol.

Results and Discussion

As proof of concept, the acylative desymmetrization of biaryl diol **1** was investigated (Table 1). Optimization studies using BTM **8** as the Lewis base in $CHCl_3$ showed isobutyric anhydride to be the optimal acylating agent (entries 1-4). While benzoic anhydride gave no acylation, acetic anhydride gave a 1:1 ratio of the mono:diester products **2** and **3**, however monoester **2** was obtained in close to racemic form (54:46 er). The use of diphenylacetic anhydride provided moderate enantioselectivity, giving **4** in 65:35 er, while isobutyric anhydride gave **6** in a promising 84:16 er. A 65:35 ratio of **6**:**7** was also observed, indicating moderate selectivity for the formation of monoester **6**. The use of alternative solvents was investigated (entries 5-7), with EtOAc and MeCN leading to preferential formation of the symmetric diacylated product **7** and PhMe showing a reduction in both ratio of mono:diester and er. The effect of temperature was probed, with improved product er observed at −40 °C. Screening a range of organic bases showed that *i*-Pr_2NEt proved optimal for providing both high product er and ratio of mono:diester products (entries 8-10). On a preparative scale, and using *i*-Pr_2NEt as the organic base, (*S*)-**6** was isolated in 32% yield and 94:6 er (entry 11), with the absolute configuration of **6** confirmed by X-ray analysis.[27] The alternative isothiourea HyperBTM **9** gave a similar product ratio but provided (*S*)-**6** in reduced er (85:15 er, entry 12). *In-situ* reaction monitoring of the enantioselective acylation of diol **1** indicated that the er of product (*S*)-**6** increased with reaction conversion (see SI for further information). In principle both reaction steps involved in the formation of monoester **6** and diester **7** could proceed enantioselectively, with product selectivity therefore dependent not only upon the selectivity of both acylation steps but also on reaction conversion to both the monoester and diester products. To probe the validity of this hypothesis, the kinetic resolution[28] (KR) of (±)-monoester **6** was performed at −40 °C in $CHCl_3$ using both BTM **8** and HyperBTM **9**. BTM **8** showed optimal selectivity, giving (*S*)-**6** in 87:13 er at 59% conversion (s = 7),[29] consistent with preferential acylation of (*R*)-monoester **6** (Scheme 1A). This selectivity factor at −40 °C corresponds to a difference in energy of 0.9 kcal/mol between the diastereomeric transition states for acylation of each enantiomer of monoester **6**. While this analysis allows for quantification of the selectivity of the second atropselective acylation event, the selectivity associated with the initial desymmetrization could not be accurately captured through experimental methods.

To gain further insight into both the desymmetrization and kinetic resolution steps, we undertook density functional theory

Table 1. Reaction optimization.

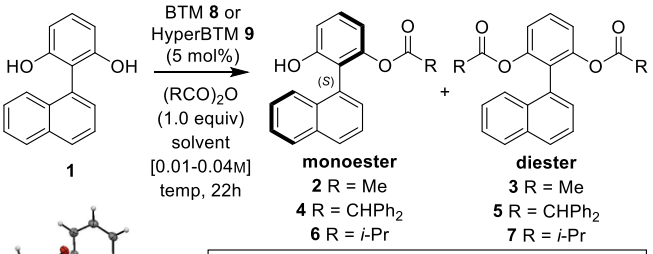

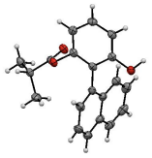

X-ray representation of (*S*)-**6**

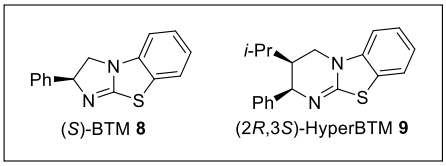

Entry	Cat.	R	Solvent	base	Temp	Ratio[a]	Yield (%)[a]	er[b]
1	**8**	Ph	$CHCl_3$	-	r.t.	-	-	-
2	**8**	Me	$CHCl_3$	-	r.t.	50:50	ND[c]	54:46
3	**8**	Ph_2CH	$CHCl_3$	-	r.t.	70:30	46	65:35
4	**8**	*i*-Pr	$CHCl_3$	-	r.t.	65:35	41	84:16
5	**8**	*i*-Pr	EtOAc	-	r.t.	30:70	15	66:34
6	**8**	*i*-Pr	PhMe	-	r.t.	50:50	30	77:23
7	**8**	*i*-Pr	MeCN	-	r.t.	30:70	17	83:17
8	**8**	*i*-Pr	$CHCl_3$	DBU	−40 °C	50:50	34	95:5
9	**8**	*i*-Pr	$CHCl_3$	DABCO	−40 °C	55:45	36	95:5
10	**8**	*i*-Pr	$CHCl_3$	*i*-Pr_2NEt	−40 °C	63:37	43	94:6
11	**8**	*i*-Pr	$CHCl_3$	*i*-Pr_2NEt	−40 °C	43:57	**(32)**	95:5
12	**9**	*i*-Pr	$CHCl_3$	*i*-Pr_2NEt	−40 °C	65:35	43	85:15

[a] Ratio of mono:diester products and yield determined by ^{1}H NMR spectroscopic analysis of the crude reaction mixture (isolated yield given in parentheses). [b] Determined by HPLC analysis using a chiral stationary phase. [c] product ratio could not be determined unambiguously using ^{1}H NMR analysis.

(DFT) computations to investigate the origins of selectivity (Scheme 1B), and also performed kinetic simulations using Kintecus[30] (Scheme 1B and Figure 2). Using DFT, geometries were optimized with M06-2X/6-31G(d) in chloroform using PCM using Gaussian09.[31] Thermochemistries were computed at −40 °C to match experiments. Final energy refinements were computed at the M06-2X/6-311++G(2df,p)/PCM(Chloroform) level.[31] These results were then further confirmed with ωB97XD/6-31G(d)/PCM(Chloroform) in Gaussian09 and again with the more accurate default grid in Gaussian16.[32] In all structures, the isobutyrate was hypothesized to initiate the acylation of the substrate alcohols by deprotonation. In the desymmetrization step, acylation to give the experimentally observed (*S*)-monoester **6** was favored by 1.7 kcal/mol (**Desymmetrization-TS-(*pro-S*)**), Scheme 1B, top left). In the following KR process, acylation of the (*R*)-monoester was favored by 1.0 kcal/mol (**Kinetic Resolution-TS-(*R*),** Scheme 1B, bottom right), quantitatively matching experiments. Notably, the relative orientations of the substrate naphthyl unit and the acylated-BTM catalyst within both favoured acylation transition state structures, **Desymmetrization-TS-(*pro-S*)** and **Kinetic Resolution-TS-(*R*)**, were relatively consistent. For the disfavoured transition state structures, **Desymmetrization-TS-(*pro-R*)** and **Kinetic**

Resolution-TS-(*S*), the same structural features also adopt similar relative positions. The relative effects of these distinct features of the favoured-TSs and disfavoured-TSs, and interrogation of the origins of selectivity, are modeled further below (Figure 3).

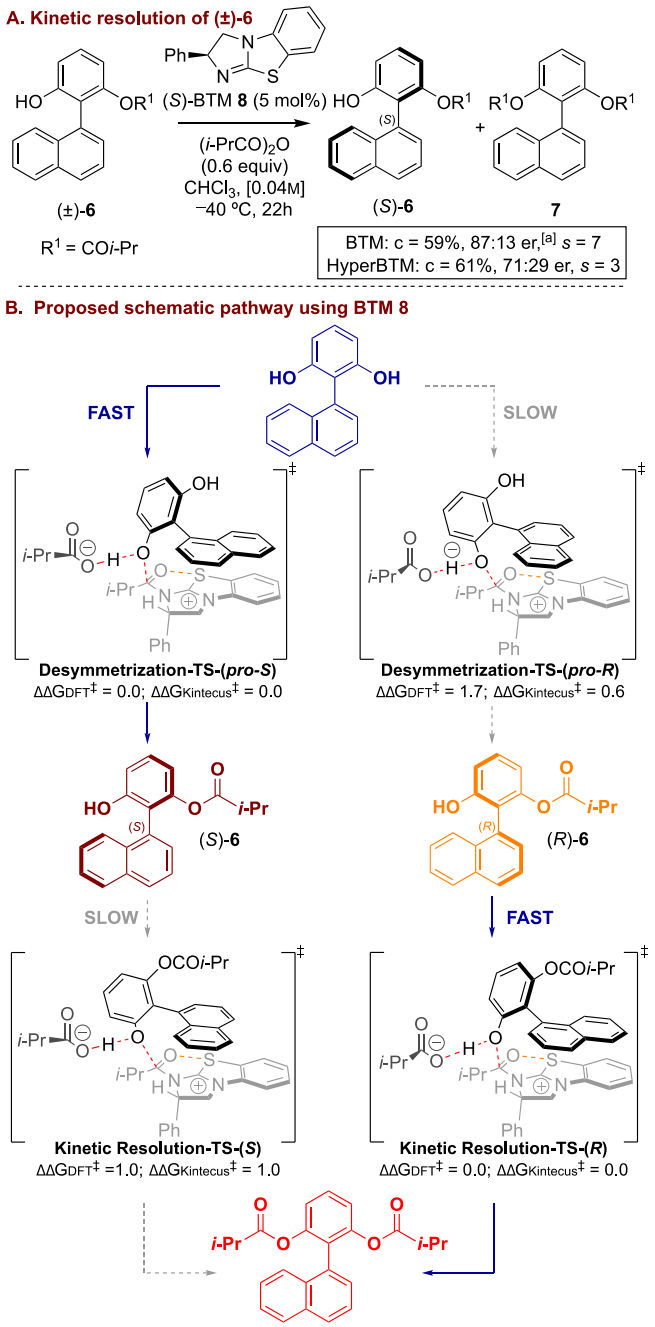

Scheme 1. Kinetic resolution of model substrate, proposed mechanistic pathway, and computed selectivities for desymmetrization and kinetic resolution processes using DFT. Calculated ΔΔG values are given in kcal/mol for both DFT and Kintecus simulation approaches for comparison. [a] (*S*):(*R*).

Kinetic simulations using Kintecus[30] allowed for analysis of both the desymmetrization and KR as discrete events. Chemical reactions were modeled in Kintecus by numerically solving for concentrations of chemical species as a function of time. The computed energies were allowed to vary to fit the experimentally observed product ratios and distributions. The resulting overall simulation profile suggests a selectivity of 0.6 kcal/mol for the desymmetrization process and 1.0 kcal/mol for the KR if the product ratios are to match the experimentally observed monoester er of 94:6 and the final ratio of monoester:diester products (Table 1, entry 10). As observed experimentally, these simulations predict that desymmetrization or kinetic resolution alone (product er = 81:19 for desymmetrization; 87:13 for KR (see SI), respectively) do not achieve the same product enantioenrichment as the combined process (er = 94:6). In effect, there is an emergent enhancement in selectivity when both processes occur concurrently as widely recognized in related desymmetrization approaches. These observations are consistent with an initial enantioselective desymmetrization of biaryl diol **1** preferentially giving (*S*)-monoester **6**, coupled with a second chiroablative kinetic resolution[25b] with preference for acylation of (*R*)-**6**, resulting in enhancement of the enantioenrichment of product (*S*)-**6** as the reaction proceeds (Figure 2).

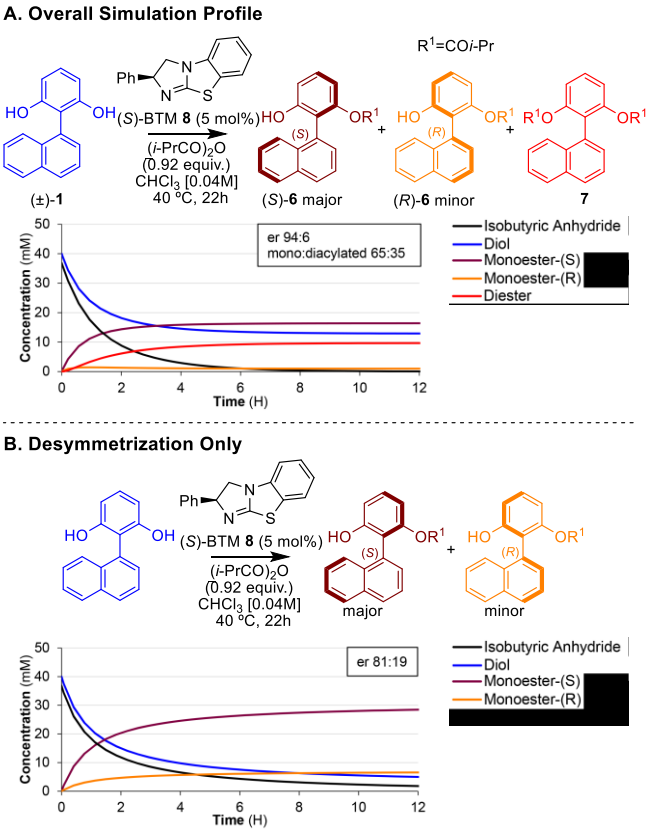

Figure 2. Kinetic simulation of title reaction (A) and desymmetrization (B). 0.92 equivalents of anhydride modelled to match experimental values, reaction conversion and product distributions.

Based on the transition state structures obtained from DFT (Scheme 1), the factors that govern the selectivity in both desymmetrization and kinetic resolution steps were further investigated (Figure 3). Simplified model systems (green atoms = H) in which the position of the substrate naphthyl group relative to the acylated-**BTM** catalyst were restrained to the TS arrangements were considered, and potential catalyst-substrate interactions modeled in isolation. Consideration of C-H•••π,[32]

cation•••π[33] and π•••π[35] interactions that are widely recognized as providing key stabilising interactions that can determine the outcome of catalytic processes,[36] actually revealed a small preference for the conformation adopted in the disfavoured TSs, **Desymmetrization-TS-(*pro-R*)** and **Kinetic Resolution-TS-(*S*)** (ΔG = –0.2 and –0.3 kcal/mol respectively; Figure 3A).

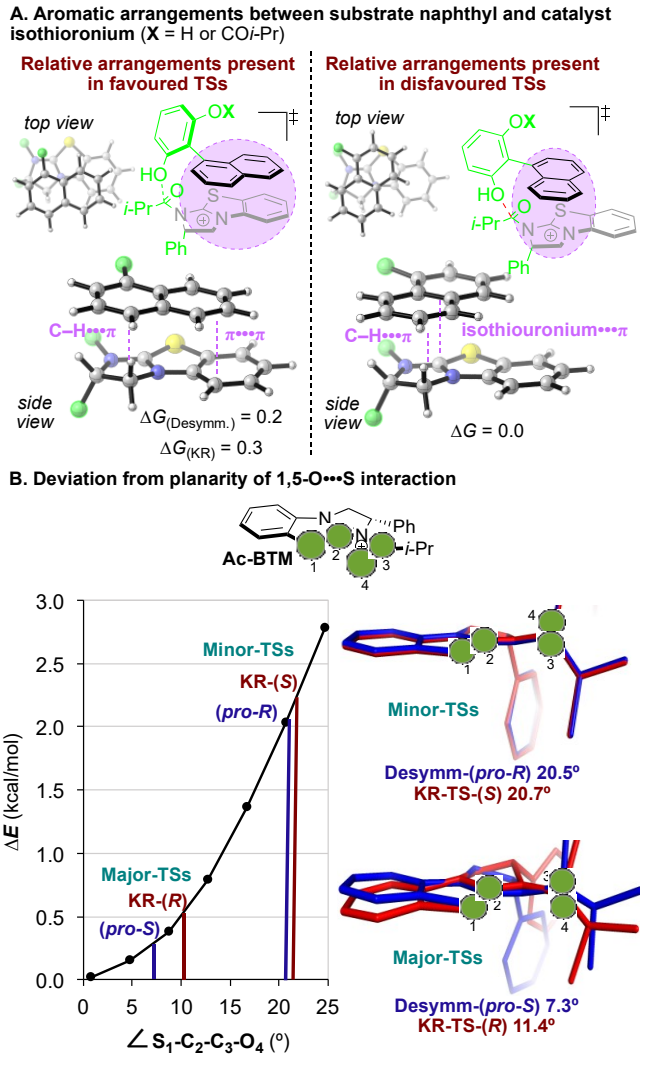

Figure 3. Exploration of origins of the reaction stereoselectivity: a) Model system used to describe C-H•••π, isothiouronium•••π and π•••π aromatic interactions (labelled green atoms constrained as H-atoms); b) Plot of ∠ S_1-C_2-C_3-O_4 vs. energy. Favoured TSs have more planar S_1-C_2-C_3-O_4 arrangements which leads to stronger O•••S interactions.

A 1,5-O•••S interaction within acylated isothioureas is widely recognized as significant for both intermediate and TS stabilization, and is maximized when these atoms are coplanar.[37] The contribution of this O•••S interaction to the overall stabilization of the four TSs calculated for the desymmetrization and kinetic resolution steps was therefore evaluated as a function of the ∠S_1-C_2-C_3-O_4 torsional angle. In the favoured **Desymmetrization-TS-(*pro-S*)** and **Kinetic Resolution-TS-(*R*)**, this angle is ~7° and 11°, respectively. By comparison, these torsional angles are significantly more distorted within the disfavoured **Desymmetrization-TS-(*pro-R*)** and **Kinetic Resolution-TS-(*S*)** (∠S_1-C_2-C_3-O_4 = ~21°). A plot of ∠S_1-C_2-C_3-O_4 vs. energy in the acylated **BTM** is shown in Figure 3B. The results reveal there is a large energetic preference for the more planar arrangements as found in the favoured **Desymmetrization-TS-(*pro-S*)** and **Kinetic Resolution-TS-(*R*)**, respectively (ΔG = 1.6; ΔG = 1.3 kcal/mol, Figure 3B).

Overall, kinetic modeling and DFT calculations have been used to understand the factors that determine selectivity in this coupled desymmetrization-kinetic resolution process. While DFT calculations overestimate ΔΔG for the desymmetrization reaction (by ~1 kcal/mol), the ΔΔG calculated for the kinetic resolution TSs closely match the experimentally-determined value. Calculation indicates that the enantioselectivity of both processes can be rationalized by maximizing a 1,5-O•••S interaction in the favoured TSs, with deviation from the preferred planarity of the S_1-C_2-C_3-O_4 torsional angle resulting in a significant loss in TS stabilization.

Further investigation probed the generality of this method through enantioselective acylation of a range of biaryl diols. Firstly, the effect of aryl substitution at C(2′) was investigated using both (*S*)-BTM **8** and (2*R*,3*S*)-HyperBTM **9** as catalysts (Scheme 2A). In all cases formation of the corresponding diester product **20-24** was observed with full product ratios given in the SI. Notable trends showed that (2*R*,3*S*)-HyperBTM **9** gave optimal enantioselectivity in each case (up to 98:2 er) to give preferentially (*R*)-configured products **15-19** in up to 54% yield. The absolute configuration within (*R*)-**19** was unambiguously confirmed by X-ray crystal structure analysis.[38] Pleasingly incorporation of both electron-donating (4-MeC_6H_4, 4-$NMe_2C_6H_4$) and electron-withdrawing (3,5-$F_2C_6H_4$) substituents within the (C2′)-aryl group was well-tolerated, with the C(2′)-4-$NMe_2C_6H_4$ substituent leading to highest mono:diester ratio (85:15) and giving **18** in excellent 98:2 er. Notably, (*S*)-BTM **8** gave enantiomeric (*S*)-configured products preferentially with moderate enantioselectivity (up to 80:20 er), despite the catalyst being in the same enantiomeric series as HyperBTM **9**. To probe the selectivity of the second acylation event, the KR of (±)-monoester **15** was carried out (Scheme 2B). Using (*S*)-BTM **8** as catalyst, acylation of (±)-monoester **15** was essentially non-selective (*s* = 1). Using (2*R*,3*S*)-HyperBTM **9**, KR of (±)-monoester **15** gave (*R*)-**15** in 82:18 er at 59% conversion (*s* = 5). These observations are consistent with a complimentary KR operating in the production of **15-19** when using HyperBTM as catalyst, with the er of monoester (*R*)-**15-19** enhanced through preferential acylation of (*S*)-**15-19** in the kinetic resolution step. The lack of selectivity in the atropselective acylation of (±)-**15** when using BTM as the catalyst indicates that the monoester product enantioselectivity derives entirely from the initial desymmetrization event, as the rate constants for acylation of each enantiomer of monoester are equal. Taken together, these observations imply that the initial enantioselective acylation event leading to desymmetrization will have opposite enantioselectivities for each catalyst, with (*S*)-BTM **8** being (*S*)-selective and (2*R*,3*S*)-HyperBTM **9** being (*R*)-selective despite both catalysts being in the same enantiomeric series.

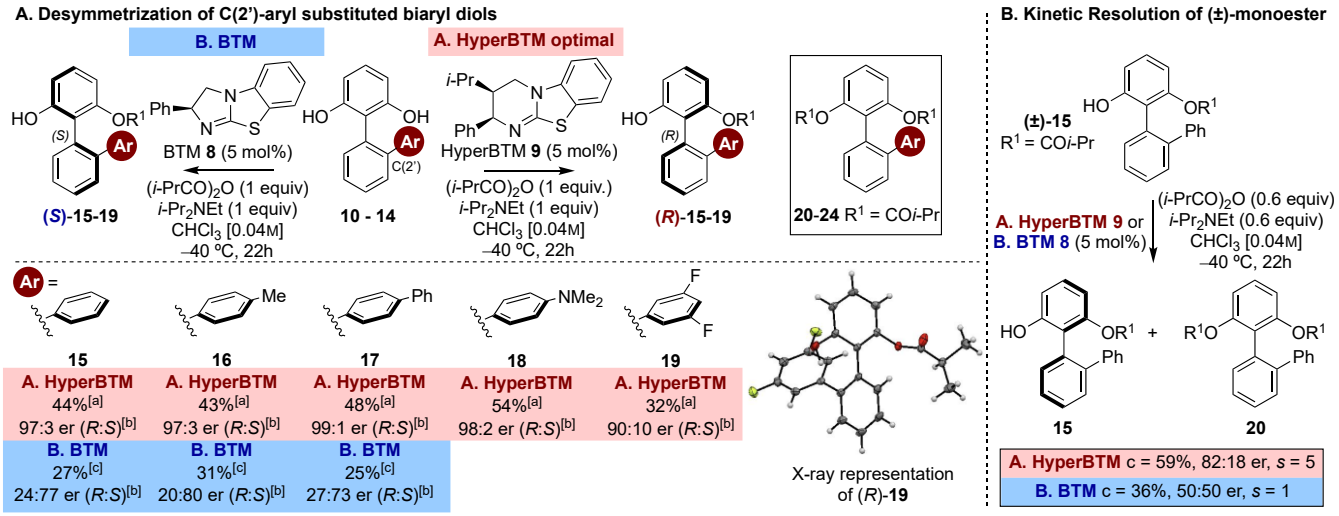

Scheme 2. Scope of C(2′)-aryl-substituted biaryls. Full details of reaction product distribution given in SI. [a] Isolated yield. [b] Determined by HPLC analysis using a chiral stationary phase. [c] Yield determined by ^{1}H NMR spectroscopic analysis of the crude reaction mixture, with an authentic sample isolated by preparative TLC for unambiguous er determination.

To further probe the scope and limitations of this process a series of C(2′)-alkyl derivatives (R = Me, Et, *i*-Pr), as well as C(2′)-amino and C(2′)-halogen (Cl, Br) substituted derivatives were prepared and evaluated (Scheme 3). In all cases formation of the corresponding diester product **39-45** was observed with full product ratios given in the SI. Within the C(2′)-alkyl series, (2*R*,3*S*)-HyperBTM **9** gave optimal enantioselectivity in each case (up to 96:4 er), to give preferentially (*R*)-configured products. Interestingly, the use of (*S*)-BTM **8** as catalyst gave the enantiomeric (*S*)-products with poor selectivity when R = methyl, but gave preferentially (*R*)-configured products with improved selectivity with increasing size of the C(2′)-alkyl substituent (up to 96:4 er for R = *i*-Pr), consistent with a steric factor dictating the preference for the (*R*)-monoester formation. Notably, for the series of C(2′)-heteroatom derivatives, (*S*)-BTM **8** proved the optimal catalyst, giving (*S*)-monoesters **32-34** in excellent (92:8 - 95:5) er in each case. The absolute configuration of **32** was confirmed by X-ray crystallographic analysis.[39] The use of (2*R*,3*S*)-HyperBTM **9** gave the opposite (*R*)-enantiomer of C(2′)-halogen-substituted monoesters **32** and **33**, however **32** and **33** were obtained in both reduced yield and er.

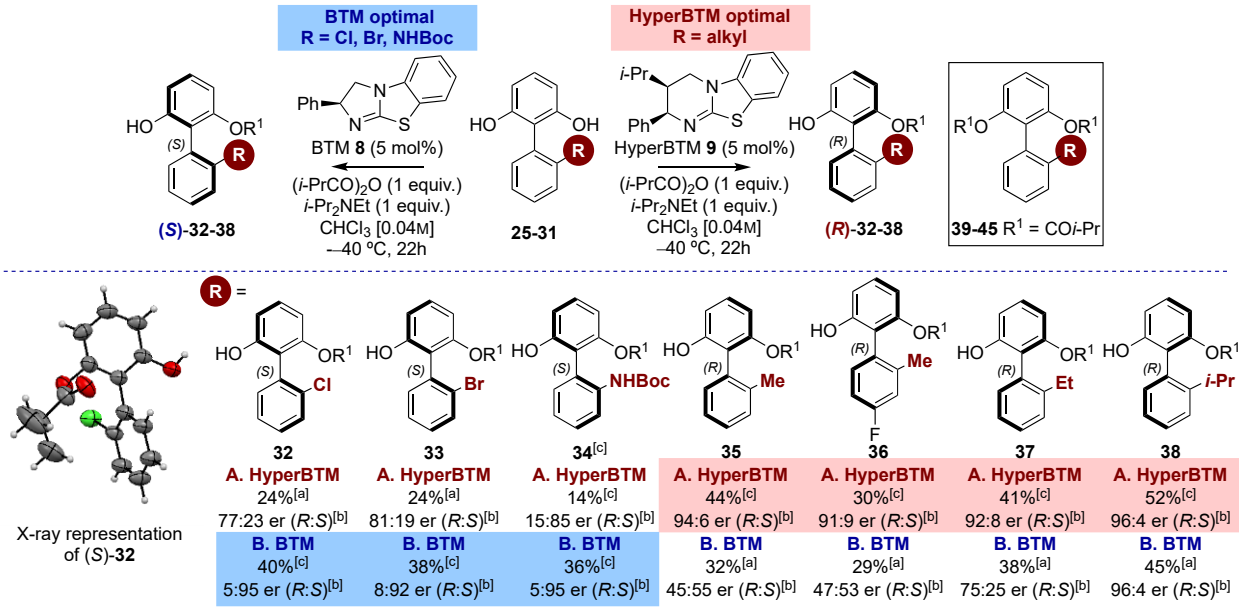

Scheme 3. Scope of C(2′)-alkyl, -halogen and -amino-substituted biaryls. Full details of reaction product distribution given in SI. [a] Yield determined by ^{1}H NMR spectroscopic analysis of the crude reaction mixture, with an authentic sample isolated by preparative TLC for unambiguous er determination. [b] Determined by HPLC analysis using a chiral stationary phase. [c] Isolated yield. [d] ratio mono:diester not determined.

Following these observations, the KR of a representative (±)-monoester from each series was carried out (Scheme 4). KR of (±)-C(2′)-Me-**36** with (2*R*,3*S*)-HyperBTM **9** proved optimal, giving (*R*)-**36** (*s* = 8 at 41% conversion), while acylation with (*S*)-BTM **8** was non-selective (*s* ≈ 1). For (±)-C(2′)-Cl-**32**, (*S*)-BTM **8** gave highest selectivity, giving (*S*)-**32** (*s* = 5 at 56% conversion), with the KR using (2*R*,3*S*)-HyperBTM-**9** significantly less selective (*s* = 2 at 50% conversion). In each case these results are consistent with the optimal catalyst in the overall desymmetrization process (HyperBTM **9** for C(2′)-alkyl derivatives; BTM **8** for C(2′)-heteroatom derivatives) preferentially acylating the minor enantiomer of the monoester, produced following desymmetrization, in a complimentary kinetic resolution to give the chiral products in enhanced enantiopurity.

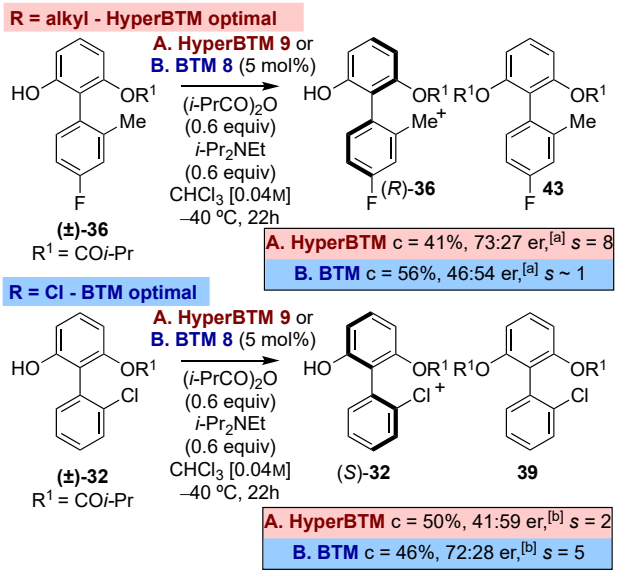

Scheme 4. Kinetic resolution of (±)-**36** and (±)-**32**. [a] ratio (*R*):(*S*) measured by HPLC analysis using a chiral stationary phase, conversion measured by ^{1}H NMR analysis of the crude reaction mixture. [b] ratio (*S*):(*R*) measured by HPLC analysis using a chiral stationary phase, conversion measured by ^{1}H NMR analysis of the crude reaction mixture.

To further test the enantiodiscriminating ability of the isothiourea catalysts, the methodology was applied to the desymmetrization of tetraorthosubstituted biaryl diol **46** (Scheme 5). Interestingly, while (2*R*,3*S*)-HyperBTM **9** gave (*S*)-**47** in 44% isolated yield and 98:2 er, high atropselectivity was also obtained with (*S*)-BTM **8**, giving (*S*)-**47** in 33% yield and 95:5 er. The absolute configuration of (*S*)-**47** was confirmed by X-ray crystallography.[40] Investigation of the KR of (±)-**47** was indicative of the operation of a complimentary kinetic resolution when using either HyperBTM **9** (*s* = 9) or BTM **8** (*s* = 9) as catalyst.

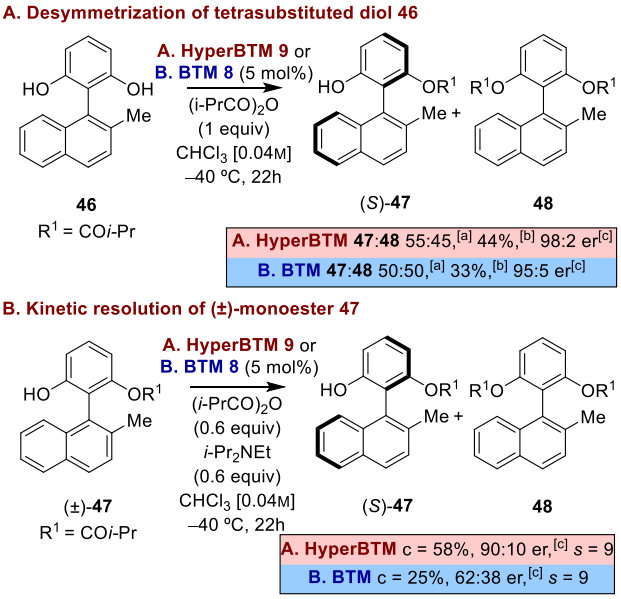

Scheme 5. Desymmetrization of tetraorthosubstituted biaryl diol **46**. [a] Conversion and product ratios measured by ^{1}H NMR analysis of the crude reaction mixture; [b] isolated yields given; [c] er measured by HPLC analysis using a chiral stationary phase.

It is clear from the changes in product configuration obtained upon variation of both the substrate and catalyst that subtle and complex differences in the interactions between acylated catalyst and substrate markedly affect the enantiorecognition events involved in both the desymmetrization and kinetic resolution steps. This makes the proposal of a global stereochemical model to explain the observed differences in selectivity challenging. Despite the complexity of this process, qualitative conclusions (excluding atropselective acylation of the naphthyl substituted examples **1** and **46**) can be drawn, in which the optimal catalyst and expected product configuration can be predicted based on the structure of the substrate (Figure 4). Biaryl substrates bearing either sp^3-hybridised C(2′)-alkyl substituents or C(2′)-aryl substituents undergo desymmetrization with highest enantioselectivity when using (2*R*,3*S*)-HyperBTM **9**, giving preferentially (*R*)-configured monoester products. Biaryl substrates bearing a C(2′)-heteroatom substituent, as well as the parent naphthyl system, undergo desymmetrization with highest enantioselectivity when using (*S*)-BTM **8** as catalyst, and lead to (*S*)-configured monoester products.

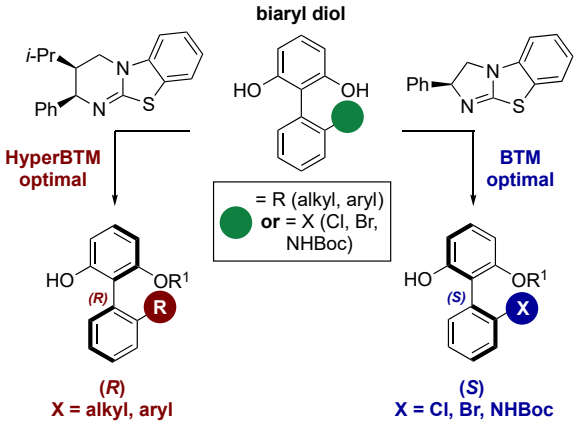

Figure 4. Summary of observed optimal catalyst and substrate combinations.

Conclusion

In summary, a range of tri- and tetra-*ortho*-substituted biaryl diols has been applied in an acylative desymmetrization process using isothiourea catalysis to produce diversely-substituted atropisomeric monoesters in high enantioselectivity. A tandem desymmetrization-kinetic resolution mechanism has been shown to be in operation and has been investigated for a number of different classes of biaryl substitution. Computation has been used to understand the factors that lead to enantiodiscrimination in this process for a model system, with maintenance of planarity to maximize a 1,5-S•••O interaction within the key acyl ammonium intermediate identified as the major feature that determines product enantioselectivity in the TS. The divergent stereoselectivity observed with variation of catalyst and substrate is indicative of subtle and complex changes in the interactions between the acylated catalyst and substrate markedly affecting the enantiorecognition events.[41]

Experimental Section

Representative general procedure for desymmetrization of a biaryl diol: The diol (1 equiv.), catalyst (5 mol%), $CHCl_3$ (0.04 M) and *i*-Pr_2NEt (1 equiv.) were added to a sealed test tube and subsequently cooled to −40 °C. Isobutyric anhydride (1 equiv.) was added, and the reaction was allowed to stir for 22 h. 1 M HCl (1mL/mmol) was added to quench the reaction, which was then allowed to warming to RT. The mixture was subsequently diluted with CH_2Cl_2 and washed with 1 M HCl, sat. $NaHCO_3$ and brine. The organic extracts were dried ($MgSO_4$), filtered, and concentrated *in vacuo* to give a residue, which was purified by flash column chromatography.

Acknowledgements

We would like to thank the Engineering and Physical Sciences Research Council, University of St Andrews, and the EPSRC Centre for Doctoral Training in Critical Resource Catalysis (CRITICAT) for financial support [Ph.D. studentship to E.M.; Grant code: EP/L016419/1]. A.D.S. thanks the Royal Society for a Wolfson Research Merit Award. We also thank the EPSRC UK National Mass Spectrometry Facility at Swansea University. PHYC gratefully acknowledges financial support from the Bert and Emelyn Christensen and Vicki & Patrick F. Stone families. PHYC, MAG, TF, ACB, and DW acknowledge the National Science Foundation (NSF, CHE-1352663). TF acknowledges Summer Fellowship Award from the department of Chemistry at OSU.

Keywords: desymmetrization • organocatalysis • isothiourea • kinetic resolution • atropisomers

[1] a) G. Bringmann, A. J. P. Mortimer, P. A. Keller, M. J. Gresser, J. Garner, M. Breuning, *Angew. Chem. Int. Ed.* **2005**, *44*, 5384–5427; b) G. Bringmann, T. Gulder, T. A. M. Gulder, M. Breuning, *Chem. Rev.* **2011**, *111*, 563–639; c) J. Wencel-Delord, A. Panossian, F. R. Leroux and F. Colobert, *Chem. Soc. Rev.*, **2015**, *44* 3418–3430; For a review on axial chirality in drug discovery, see: d) S. R. LaPlante, P. J. Edwards, L. D. Fader, A. Jakalian, O. Hucke, *ChemMedChem* **2011**, *6*, 505–513.

[2] a) P. Renzi, *Org. Biomol. Chem.* **2017**, *15*, 4506–4516; b) B. Zilate, A. Castrogiovanni, C. Sparr, *ACS Catal.* **2018,** *8*, 2981–2988; c) Y.-B. Wang, B. Tan, *Acc. Chem. Res.* **2018**, *51*, 534–547.

[3] J. Yin, S. L. Buchwald, *J. Am. Chem. Soc.* **2000**, *122*, 12051–12052.

[4] G. Xu, W. Fu, G. Liu, C. H. Senanayake, W. Tang, *J. Am. Chem. Soc.* **2014**, *136*, 570–573.

[5] For selected reviews concerning DKR see a). F. F. Huerta, A. B. E. Mindis, J-E. Backvall, *Chem. Soc. Rev.* **2001**, 30, 321–331; b. O. Verho, J-E. Backvall, *J. Am. Chem. Soc.* **2015**, *137*, 3996–4009.

[6] J. L. Gustafson, D. Lim, S. J. Miller, *Science* **2010**, *328*, 1251–1255.

[7] S. Staniland, R. W. Adams, J. J. W. McDouall, I. Maffucci, A. Contini, D. M. Grainger, N. J. Turner, J. Clayden, *Angew. Chem. Int. Ed.* **2016**, *55*, 10755–10759.

[8] Selected examples: a) A. Fugard, A. Lahdenperä, A. Mekareeya, J. Tan, R. Paton, M. D. Smith, *Angew. Chem. Int. Ed.* **2019**, *58*, 2795–2798; b) G. Bringmann, T. Pabst, P. Henschel, J. Kraus, K. Peters, E. M. Peters, D. S. Rycroft, J. D. Connolly, *J. Am. Chem. Soc.* **2000**, *122*, 9127–9133; c) K. Mori, T. Itakura, T. Akiyama, *Angew. Chem. Int. Ed.* **2016**, *55*, 11642–11646; d) C. Yu, H. Huang, X. Li, Y. Zhang, W. Wang, *J. Am. Chem. Soc.* **2016**, *138*, 6956–6959.

[9] For selected reviews concerning enantioselective desymmetrisation see a). M. C. Willis, J. *Chem. Soc. Perkin Trans 1*, **1999**, 1765-1784; b). X-P. Zeng, Z-H. Cao, Y-H. Wang, F. Zhou, J. Zhou, *Chem. Rev.* **2016,** *116*, 7330–7396; c). A. Borissov, T. Q. Davies, S. R. Ellis, T. A. Fleming, M. S. W. Richardson, D. J. Dixon, *Chem. Soc. Rev.* **2016**, *45*, 5474–5540; d) J. Meraud, M. Candy, J.-M. Pons and C. Bressy, *Synthesis*, **2017**, *49*, 1938–1954.

[10] Selected examples: a) S. Shirakawa, X. Wu, S. Liu, K. Maruoka, *Tetrahedron* **2016**, *72*, 5163–5171; b) T. Osako, Y. Uozumi, *Org. Lett.* **2014,** *16*, 5866–5869.

[11] K. Mori, Y. Ichikawa, M. Kobayashi, Y. Shibata, M. Yamanaka, T. Akiyama, *J. Am. Chem. Soc.* **2013**, *135*, 3964–3970.

[12] T. Kamikawa, Y. Uozumi, T. Hayashi, *Tetrahedron Lett.* **1996**, *37*, 3161–3164.

[13] T. Kamikawa, T. Hayashi, *Tetrahedron* **1999**, *55*, 3455–3466.

[14] R. J. Armstrong, M. D. Smith, *Angew. Chem. Int. Ed.* **2014**, *53*, 12822–12826.

[15] G. Ma, M. P. Sibi, *Chem. Eur. J.* **2015**, *21*, 11644–11657.

[16] G. Ma, C. Deng, J. Deng, M. P. Sibi, *Org. Biomol. Chem.* **2018**, *16*, 3121–3126.

[17] S. Lu, S. B. Poh, Y. Zhao, *Angew. Chem. Int. Ed.* **2014**, *53*, 11041–11045.

[18] S. Qu, M. Greenhalgh, A. D. Smith, *Chem. Eur. J.* **2019**, *25*, 1064-1075. For other examples of enantioselective acylation processes developed within our group see

[19] Desymmetrization of a limited number of biaryl diesters using enzymatic deacylation has been reported For example see: a) T. Matsumoto, T. Konegawa, T. Nakamura, K. Suzuki, *Synlett,* **2002**, 0122–0124; b) S. Yamaguchi, N. Takahashi, D. Yuyama, K. Sakamoto, K. Suzuki, T. Matsumoto, *Synlett* **2016**, *27*, 1262–1268; c) M. Ochiai, Y. Akisawa, D. Kajiyama, T. Matsumoto, *Synlett* **2019**, *30*, 557–562.

[20] S. Lu, S. B. Poh, Z Rong, Y. Zhao, *Org. Lett.* **2019**, *21*, 6169–6172.

[21] J. Merad, J. Pons, O. Chuzel, C. Bressy, *Eur. J. Org. Chem.* **2016**, 5589–5610.

[22] A. S. Burns, A. J. Wagner, J. L. Fulton, A. Zakarian, S. D. Rychnovsky, *Org. Lett.* **2017**, 19, 2953–2956.

[23] a) V. B. Birman, X. Li, *Org. Lett.* **2006**, *8*, 1351–1354; b) X. Li, H. Jiang, E. W. Uffman, L. Guo, Y. Zhang, X. Yang, V. B. Birman, *J. Org. Chem.* **2012**, *77*, 1722–1737; c) Q. Hu, H. Zhou, X. Geng, P. Chen, *Tetrahedron* **2009**, *65*, 2232–2238; d) P. Chen, Y. Zhang, H. Zhou, Q. Xu, *Acta Chim. Sinica* **2010**, *68*, 1431; e) I. Shiina, K. Nakata, K. Ono, M. Sugimoto, A. Sekiguchi, *Chem. Eur. J.* **2010**, *16*, 167–172; f) I. Shiina, K. Ono, K. Nakata, *Chem. Lett.* **2011**, *40*, 147–149; g) K. Nakata, K. Gotoh, K. Ono, K. Futami, I. Shiina, *Org. Lett.* **2013**, *15*, 1170–172; h) I. Shiina, K. Ono, T. Nakahara, *Chem. Commun.* **2013**, *49*, 10700–10702; i) D. Belmessieri, C. Joannesse, P. A. Woods, C. MacGregor, C. Jones, C. D. Campbell, C. P. Johnson, N. Duguet, C. Concellón, R. A. Bragg, A. D. Smith, *Org. Biomol. Chem.* **2011**, *9*, 559–570; j) S. F. Musolino, O. S. Ojo, N. J. Westwood, J. E. Taylor, A. D. Smith, *Chem. Eur. J.* **2016**, *22*, 18916–18922; k) S. Harrer, M. D. Greenhalgh, R. M. Neyappadath, A. D. Smith, *Synlett*, **2019**, *30*, 1555–1560.

[24] M. D. Greenhalgh, S. M. Smith, D. M. Walden, J. E. Taylor, Z. Brice, E. R. T. Robinson, C. Fallan, D. B. Cordes, A. M. Z. Slawin, H. C. Richardson, M. A. Groves, P. H.-Y. Cheong, A. D. Smith, *Angew. Chem. Int. Ed.* **2018**, *57*, 3200–3206.

[25] a) V. B. Birman, H. Jiang, X. Li, *Org. Lett.* **2007**, *9*, 3237–3240; b) J. Merad, P. Borkar, T. B. Yenda, C. Roux, J.-M. Pons, J.-L. Parrain, O. Chuzel, C. Bressy, *Org. Lett*. **2015**, *17*, 2118–2121; c) J. Merad, P. Borkar, F. Caijo, J.-M. Pons, J.-L. Parrain, O. Chuzel, C. Bressy, *Angew. Chem. Int. Ed.* **2017**, *56*, 16052–10656; For a review of the acylative desymmetrization of *meso*-diols, see: d) Á. Enríquez-García, E. P. Kündig, *Chem. Soc. Rev*. **2012**, *41*, 7803–7831.

[26] a) J. P. Vigneron, M. Dhaenens, A. Horeau, *Tetrahedron* **1973**, *29*, 1055–1059; b) W. Kroutil, A. Kleewein, K. Faber, *Tetrahedron: Asymmetry*, **1997**, *8*, 3251–3261;

[27] CCDC 1952952 (**6**) contains the supplementary crystallographic data for this paper. These data can be obtained free of charge from The Cambridge Crystallographic Data Centre.

[28] a) M. D. Greenhalgh, J. E. Taylor, A. D. Smith, *Tetrahedron*, **2018**, *74*, 5554-5560; For derivation of *s* see: b) H. B. Kagan, J. C. Fiaud, *Top. Stereochem.* **1988**, *18*, 249–330.

[29] Selectivity factor (*s*) is the most commonly used metric to report the efficiency of a KR, and is defined as the rate constant for the fast reacting enantiomer divided by the rate constant for the slow reacting enantiomer ($s = k_{fast}/k_{slow}$). See references [26a] and [26b] for more details. Based on our previous work and estimations of error in enantioselective acylation reactions *s* is given to the closest integer in this manuscript.

[30] J. C. Ianni, *Computational Fluid and Solid Mechanics*, **2003**, K. J. Bathe, Ed., Elsevier Science Ltd: Oxford, pp. 1368–1372

[31] a) Y. Zhao, D. G. Truhlar, *Theor Chem Account* **2008**, *120*, 215–241; b) W. J. Hehre, R. Ditchfield, J. A. Pople, *J. Chem. Phys.*, **1972**, *56*, 2257–2261; c) J. Tomasi, B. Mennucci, R. Cammi, *Chem. Rev.*, **2005**, *105*, 2999–3093; d) J. R. Cheeseman, G. W. Trucks, T. A. Keith and J. Frisch, *J. Chem. Phys.* **1996**, *104*, 5497–5509; Gaussian 09, Revision D.01, M. J. Frisch, G. W. Trucks, H. B. Schlegel, G. E. Scuseria, M. A. Robb, J. R. Cheeseman, G. Scalmani, V. Barone, G. A. Petersson, H. Nakatsuji, X. Li, M. Caricato, A. Marenich, J. Bloino, B. G. Janesko, R. Gomperts, B. Mennucci, H. P. Hratchian, J. V. Ortiz, A. F. Izmaylov, J. L. Sonnenberg, D. Williams-Young, F. Ding, F. Lipparini, F. Egidi, J. Goings, B. Peng, A. Petrone, T. Henderson, D. Ranasinghe, V. G. Zakrzewski, J. Gao, N. Rega, G. Zheng, W. Liang, M. Hada, M. Ehara, K. Toyota, R. Fukuda, J. Hasegawa, M. Ishida, T. Nakajima, Y. Honda, O. Kitao, H. Nakai, T. Vreven, K. Throssell, J. A. Montgomery, Jr., J. E. Peralta, F. Ogliaro, M. Bearpark, J. J. Heyd, E. Brothers, K. N. Kudin, V. N. Staroverov, T. Keith, R. Kobayashi, J. Normand, K. Raghavachari, A. Rendell, J. C. Burant, S. S. Iyengar, J. Tomasi, M. Cossi, J. M. Millam, M. Klene, C. Adamo, R. Cammi, J. W. Ochterski, R. L. Martin, K. Morokuma, O. Farkas, J. B. Foresman, and D. J. Fox, Gaussian, Inc., Wallingford CT, **2009**.

[32] a) J. Chai, M. Head-Gordon, *J. Chem. Phys.* **2008**, *10*, 6615–6620; b) A. N. Bootsma, S. Wheeler, *ChemRxiv* **2019**. Gaussian 16, Revision A.03, M. J. Frisch, G. W. Trucks, H. B. Schlegel, G. E. Scuseria, M. A. Robb, J. R. Cheeseman, G. Scalmani, V. Barone, G. A. Petersson, H. Nakatsuji, X. Li, M. Caricato, A. V. Marenich, J. Bloino, B. G. Janesko, R. Gomperts, B. Mennucci, H. P. Hratchian, J. V. Ortiz, A. F. Izmaylov, J. L. Sonnenberg, D. Williams-Young, F. Ding, F. Lipparini, F. Egidi, J. Goings, B. Peng, A. Petrone, T. Henderson, D. Ranasinghe, V. G. Zakrzewski, J. Gao, N. Rega, G. Zheng, W. Liang, M. Hada, M. Ehara, K. Toyota, R. Fukuda, J. Hasegawa, M. Ishida, T. Nakajima, Y. Honda, O. Kitao, H. Nakai, T. Vreven, K. Throssell, J. A. Montgomery, Jr., J. E. Peralta, F. Ogliaro, M. J. Bearpark, J. J. Heyd, E. N. Brothers, K. N. Kudin, V. N. Staroverov, T. A. Keith, R. Kobayashi, J. Normand, K. Raghavachari, A. P. Rendell, J. C. Burant, S. S. Iyengar, J. Tomasi, M. Cossi, J. M. Millam, M. Klene, C. Adamo, R. Cammi, J. W. Ochterski, R. L. Martin, K. Morokuma, O. Farkas, J. B. Foresman, and D. J. Fox, Gaussian, Inc., Wallingford CT, **2016**.

[33] For a comprehensive review see M. Nishio, *Phys. Chem. Chem. Phys*. **2011**, *13*, 13873–13900.

[34] For useful reviews and accounts see a) For a review on nitrogen cation-π interactions in organocatalysis see: S. Yamada, J. S. Fossey, *Org. Biomol. Chem.* **2011**, *9*, 7275–7281; b) C. R. Kennedy, S. Lin, E. N. Jacobsen, *Angew. Chem. Int. Ed*. **2016**, *55*, 12596–12624; c) D. A. Dougherty, *Acc. Chem. Res*. **2013**, *46*, 885–893; d) S. Yamada, *Chem. Rev.* **2018**, *118*, 11353-11432. For selected applications in isothiourea mediated catalysis see e) T. H. West, D. M. Walden, J. E. Taylor, A. C. Brueckner, R. C. Johnston, P. H.-Y. Cheong, G. C. Lloyd-Jones, A. D. Smith, *J. Am. Chem. Soc.* **2017**, *139*, 4366–4375; f) S. S. M. Spoehrle, T. H. West, J. E. Taylor, A. M. Z. Slawin, A. D. Smith, *J. Am. Chem. Soc.* **2017**, *139*, 11895–11902; g) K. Kasten, A. M. Z. Slawin, A. D. Smith, *Org. Lett.* **2017**, *19*, 5182–5185.

[35] For an interesting review see C. R. Martinez, B. L. Iverson, *Chem. Sci*. **2012**, *3*, 2191–2201.

[36] For selected overviews see a) J. Neel, M. J. Hilton, M. S. Sigman, F. D. Toste, Nature, **2017**, *543*, 637–646; b) R. R. Knowles, E. N. Jacobsen and D. W. C. Macmillan, *Proc. Nat. Acad. Sci*. **2010**, *107*, 20678–20685.

[37] Non-covalent S···O interactions have recognized importance in medicinal chemistry: a) B. R. Beno, K.-S. Yeung, M. D. Bartberger, L. D. Pennington, N. A. Meanwell, *J. Med. Chem.*, **2015**, *58*, 4383–4438; b) X. Zhang, Z. Gong, J. Li, T. Lu, *J. Chem. Inf. Model.* **2015**, *55*, 2138–2153; For selected discussions of S···O interactions in isothiourea-catalyzed reactions, see reference 22c and c) V. B. Birman, X. Li, Z. Han, *Org. Lett.* **2007**, *9*, 37–40; d) P. Liu, X. Yang, V. B. Birman, K. N. Houk, *Org. Lett.* **2012**, *14*, 3288–3291; e) E. R. T. Robinson, D. M. Walden, C. Fallan, M. D. Greenhalgh, P. H.-Y. Cheong, A. D. Smith, *Chem. Sci.* **2016**, *7*, 6919–6927;For an excellent discussion on the origin of chalcogen-bonding interactions see: f) D. J. Pascoe, K. B. Ling, S. L. Cockcroft, *J. Am. Chem. Soc.* **2017**, *139*, 15160–15167.

[38] CCDC 1952953 (**19**) contains the supplementary crystallographic data for this paper. These data can be obtained free of charge from The Cambridge Crystallographic Data Centre.

[39] CCDC 1952954 (**32**) contains the supplementary crystallographic data for this paper. These data can be obtained free of charge from The Cambridge Crystallographic Data Centre.

[40] CCDC 1952955 (**47**) contains the supplementary crystallographic data for this paper. These data can be obtained free of charge from The Cambridge Crystallographic Data Centre.

[41] The research data underpinning this publication can be found at https://doi.org/10.17630/b0b1a7d6-ba1e-45a4-88c0-2aba9ed4ef9b

Entry for the Table of Contents (Please choose one layout)

Layout 1:

RESEARCH ARTICLE

Atropselective acylation of symmetric biaryl diols using isothiourea catalysis leads to chiral biaryls with high er. Computational and synthetic studies indicate this process consists of two successive enantioselective reactions with an initial desymmetrization coupled with a chiroablative kinetic resolution. Computation indicates that maintenance of planarity to maximize a 1,5-S•••O interaction within the key acyl ammonium as the major feature in determining enantioselectivity.

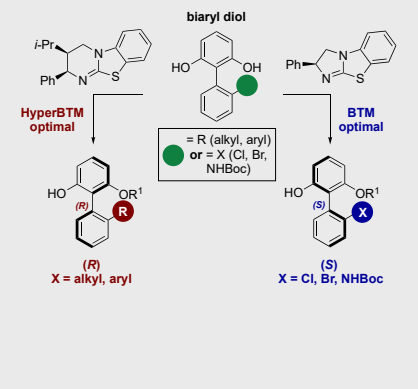

Elizabeth S. Munday, Markas A. Grove, Taisiia Feoktistova, Alexander C. Brueckner, Daniel Walden, Alexandra M. Z Slawin, Andrew D. Campbell, Paul Ha-Yeon Cheong and Andrew D. Smith**

Page No. – Page No.

Isothiourea-Catalyzed Atropselective Acylation of Biaryl Phenols via Sequential Desymmetrization / Kinetic Resolution